A NUMERICAL STUDY USING MIXTURES OF WATER - ETHYLENE GLYCOL BASED NANOFLUIDS ON LAMINAR HEAT TRANSFER OF AN ANNULUS

Elif Büyük ÖĞÜT
Kocaeli University, Hereke MYO, 41800 Hereke, Kocaeli
elif.ogut@kocaeli.edu.tr

Koray ÖZDEMİR
Kocaeli University Institute of Science, Kocaeli
koray.ozdemir@outlook.com.tr

Halil İbrahim SARAÇ
Kocaeli University, Mechanical Engineering Department, Kocaeli
sarac@kocaeli.edu.tr

Abstract: In this study, developing laminar flow and heat transfer behaviour of ethylene glycol (EG) and water mixture based SiO_2 nanofluids in an annulus have been numerically investigated. A constant heat flux was applied to the inner walls of the annulus with 100 W / m^2. Water 100% - EG 0%, water 50% - EG 50% and water 0% - EG 100% mixtures have been utilized as the base fluids. SiO_2 nanoparticles have been used with d = 20 nm and volume fractions ϕ =0%-4%. The Reynolds number varies from 200 to 1000. The physical model of the test section mainly consists of two concentric horizontal cylinders that form an annular space ranging from two interconnected elliptical tubes with axis ratio ($r_1/r_2=1/2$) placed at the centre of a circular cylinder with major radius of $2r_2$ with the length of 1 m. Governing equations have been solved with Ansys Fluent programme. The velocity distribution, temperature contours, average Nusselt number and thermal-hydraulic performance have been analysed and presented. The effects of nanofluids have been examined on heat and flow fields and it has been observed that the heat transfer increases together with the nanoparticle volume concentration. When the nanofluid is used in a forced convection, the amount of heat transfer increases as the Reynolds number increases. The highest value of the average Nusselt number was obtained in the EG based nanofluid with ϕ=4% and Re=1000 as 29.14, and the lowest value was obtained in the water-based nanofluid with ϕ=4% and Re=200 as 5.61. Results show that the use of nanofluid in the annulus channel increases the thermal performance of systems.

Key words: Elliptic annulus, heat transfer, nanofluid, CFD.

Introduction

Heat transfer describes the exchange of thermal energy, between physical structures relying at the temperature and pressure, by means of dissipating heat. The essential modes of heat transfer are conduction, convection and radiation. Engineers also consider the transfer of mass of differing chemical species, either cold or hot, to attain heat transfer. Convection is concerned with the transfer of thermal energy in a moving fluid (liquid or gas). It's far ruled by means of two phenomena: the movement of energy because of molecular vibrations and the massive-scale movement of fluid particles (2018). In preferred, convection is of sorts, forced convection and free convection. Forced convection takes place while a fluid is forced to flow. For example, a fan blowing air over a heat exchanger is an instance of forced convection. In free convection, the majority fluid movement is due to buoyancy effects. As an example, a vertical heated plate surrounded by using quiescent air causes the air surrounding it to be heated. Due to the fact hot air has a decrease density than cold air, the hot air rises. The void is crammed by using cold air and the cycle continues. Mixed convection heat transfer exists whilst natural convection currents are the identical order of importance as pressured flow velocities. The time period "mixed Convection" is also used, and the flows may be inner or external to a bounding floor (Joye, 2003). Annular pipe flow is regularly encountered in engineering applications which includes heat exchangers, combustion systems, and drilling operations inside the oil and gas industry. Furthermore, annular pipe flow gives a perception into the trouble of turbulent flows with curved walls. Commonly, flow in a flat channel generates a symmetrical velocity profile and makes the positions of zero shear stress and most velocity coincident. However, the flow in a concentric annular channel does not result in a symmetric velocity profile. The asymmetric velocity profiles end result from the interaction of flow zones with different Reynolds numbers primarily based at the outer and inner cylinder radii. In the case of annular pipe flow, boundary layers exist and each has a different distribution of turbulent quantities. Furthermore, pipe and channel flows are the restricting cases of annular pipe flow. For a high radius ratio, the

profiles of turbulent quantities near the internal cylinder are just like those of the turbulent channel flow approximately a cylinder in axial go with the flow. Alternatively, the profiles near the outer wall are similar to those of turbulent pipe flow. Notwithstanding the importance of the hassle, the numerical simulation of turbulent pipe flow has received less interest than plane channel flow due to the numerical difficulties in precisely treating curved geometries (Ghaffari Motlagh, Ahn, Hughes, & Calo, 2013). Conceptually, investigation of the heat transfer enhancement in annuluses is vital. The heat transfer enhancement technology has been stepped forward and broadly used inside the heat exchanger applications. One of the extensively used heat transfer enhancement technique is placing distinct fashioned elements with unique geometries in channel flow (Khaled, 2007; Mokhtari Moghari, Akbarinia, Shariat, Talebi, & Laur, 2011; Shoji, Sato, & Oliver, 2003; Zimparov, 2001). The tubes of elliptic cross section have drawn precise interest due to the fact that they were determined to create less resistance to the cooling fluid which ends up in less pumping power (Velusamy, Garg, & Vaidyanathan, 1995). Velusamy and Garg (Velusamy & Garg, 1996) have studied mixed and forced convection fluid flow in ducts with elliptic and circular cross sections. They found that irrespective of the value of the Rayleigh range, the ratio of friction issue at some stage in mixed convection to the corresponding value at some stage in forced convection is low in elliptical ducts in comparison to that in a circular duct in addition to the ratio of Nusselt quantity to friction factor is higher for elliptic ducts in comparison to that for a circular duct. Notwithstanding the truth that the secondary flow in elliptical ducts is very small compared to the move sensible bulk flow, secondary motions play a substantial role by means of cross-flow moving momentum, heat and mass. On the other hand, the principle benefit of the use of elliptic ducts than circular ducts is the boom of heat transfer coefficient (Sakalis, Hatzikonstantinou, & Kafousias, 2001). As a result, heat transfer enhancement in these devices is crucial, nanofluids usage may be play powerful roles to increase heat transfer coefficient. in the course of the beyond decade technology to make particles in nanometre dimensions changed into progressed and a new type of strong–liquid mixture this is referred to as nanofluid, was seemed (Choi, S. U. S., n.d.). The nanofluid is an increase form of fluid containing small quantity of nanoparticles (usually less than 100 nm) which might be uniformly and stably suspended in a liquid. The dispersion of a small amount of solid nanoparticles in conventional fluids inclusive of water or EG modifications their thermal conductivity remarkably. Thermal conductivity of nanofluids has been measured through several authors with specific nanoparticle extent fraction, material and dimension in several base fluids and all findings show that thermal conductivity of nanofluid is higher than the bottom fluids. Among them, Lee et al. (Lee, Choi, Li, & Eastman, 1999) established that oxide ceramic nanofluids including CuO or Al_2O_3 nanoparticles in water or ethylene-glycol show off more advantageous thermal conductivity. As an instance, the usage of Al_2O_3 nanoparticles having suggested diameter of thirteen nm at 4.three% quantity fraction expanded the thermal conductivity of water below stationary conditions via 30% (Masuda, Ebata, & Teramae, 1993). However, large particles with an average diameter of 40 nm led an increase of less than 10% (Choi, S. U. S., n.d.)Distinctive ideas were proposed to provide an explanation for this enhancement in heat transfer. Xuan and Li (Xuan, 2000) and Xuan and Roetzel (Xuan & Roetzel, 2000) have recognized two reasons of improved heat transfer with the aid of nanofluids: the increased thermal dispersion because of the chaotic motion of nanoparticles that accelerates energy exchanges inside the fluid and the enhanced thermal conductivity of nanofluid. Then again, Keblinski et al. (Keblinski, Phillpot, Choi, & Eastman, 2002) have studied 4 possible mechanisms that contribute to the increase in nanofluid heat transfer: Brownian motion of the particles, molecular-stage layering of the liquid/particle interface, ballistic heat transfer in the nanoparticle and nanoparticle clustering. Similarly to Wang et al., (Wang, Xu, & Choi, 1999) they showed that the effects of the interface layering of liquid molecules and nanoparticles clustering could offer paths for speedy heat transfer. These days, Izadi et al. (Izadi, Behzadmehr, & Jalali-Vahid, 2009) studied the hydrodynamic and thermal behaviours of an Al_2O_3/water nanofluid flowing through an annulus underneath a laminar glide regime. In their observe, a single-section version was used for nanofluid simulation. The effects indicated that the particle volume concentration has no considerable effect on the dimensionless axial speed, however affects the temperature subject and increases the heat transfer coefficient. Mirmasoumi and Behzadmehr (Mirmasoumi & Behzadmehr, 2008) investigated the laminar mixed convection heat transfer of Al_2O_3/water nanofluid flowing thru a horizontal tube numerically. A two-phase aggregate model was used to explain the hydrodynamic and thermal behaviour of the nanofluid. The numerical results indicated that inside the completely developed region the particle concentration has insignificant results on the hydrodynamic parameters, whilst it has crucial results at the thermal parameters. Furthermore, the consequences showed that nanoparticle concentration is higher at the lowest of the take a look at tube and on the close to wall region. However, Akbarinia (Akbarinia, 2008) and Akbarinia and Behzadmehr (Akbarinia & Behzadmehr, 2007) numerically investigated the fully developed laminar mixed convection of Al_2O_3/water nanofluid flowing through a horizontal curved tube. In their research, 3-dimensional elliptic governing equations were used. The results of the buoyancy pressure, centrifugal pressure and particle concentration on the heat transfer performance have been provided. The results confirmed that the particle concentration has no direct impact on the secondary flow, axial velocity and pores and skin friction coefficient. However, while the buoyancy pressure is more important than the centrifugal pressure, the impact of particle concentration at the entire fluid temperature can affect the hydrodynamic parameters. Furthermore, the consequences also indicated that the buoyancy force decreases the Nusselt number while the

particle concentration has a high quality impact on the heat transfer enhancement and on the skin friction reduction. In this paper, a numerical investigation on heat transfer performance and flow fields of different nanofluids flows through elliptic annulus in a laminar and turbulent flow regimes. The three-dimensional continuity, Navier–Stokes and energy equations are solved by using finite volume method (FVM) and the SIMPLE algorithm scheme is applied to examine the effects of laminar and turbulent flow on heat transfer characteristics. Dawood et al (Dawood, Mohammed, Sidik, & Munisamy, 2015) evaluated the effects of four different types of nanoparticles, Al_2O_3, CuO, SiO_2 and ZnO, with different volume fractions (0.5–4%) and diameters (25–80 nm) under constant heat flux boundary condition using water as a base fluid The Reynolds number of laminar flow was in the range of $200 \leq Re \leq 1500$, while for turbulent flow it was in the range of $4000 \leq Re \leq 10,000$. The results have shown that SiO_2–water nanofluid has the highest Nusselt number, followed by ZnO–water, CuO–water, Al2O3–water, and lastly pure water. They showed that the Nusselt number for all cases increases with the volume fraction but it decreases with the rise in the diameter of nanoparticles. In all configurations, the Nusselt number increases with Reynolds number. In their study, it is found that the glycerine–SiO_2 shows the best heat transfer enhancement compared with other tested base fluids.

As seen in those and/or similar works, heat transfer mechanisms in annulus can be very complicated and this geometry might be regarded in many commercial set up. Consequently, the existing work targets to investigate some behaviours of nanofluid flow in an elliptic annulus. As a result, the results of volume fraction and specific base fluids comprised of water and ethylene glycol mixtures on the thermodynamics and hydrodynamics parameters of a 3-D laminar forced convection through an elliptic concentric annulus were studied. Effect of water and ethylene glycol volume fractions were addressed as EG fractions ranges from 0% to 100% with a 50% increment. This research covers Reynolds range within the range of $200 \leq Re \leq 1000$ (laminar) with a diameter of 20 nm silicon oxide (SiO_2) nanoparticle. Different volume fractions SiO_2 nanoparticles within the base fluids ranged from 0% to 4% were also considered. Outcomes of pursuits which include Nusselt wide variety for laminar forced convection heat transfer in an elliptic annulus were stated to illustrate the impact of nanofluids on these parameters.

Physical Model

The physical model of the test section mainly consists of two concentric horizontal cylinders used to form an annular space ranging from an integrated double elliptical tube placed at the center of a circular cylinder. The outer cylinder was made from aluminium of 20 mm outer diameter, 1 mm thickness, and 500 mm length. The inner elliptic cylinder was made of aluminium with a major radius (r_2) of 10 mm and a length of 500 mm that had an axis ratio ($r_1/r_2 = 1/2$). The internal wall of the annular space (elliptic tube surface) was maintained under constant heat flux (q_h).Whereas the external wall of the annular space (circular cylinder surface) was kept insulated (T_c). The schematic diagram of the annular space under consideration and coordinate system are shown in Figure 1.
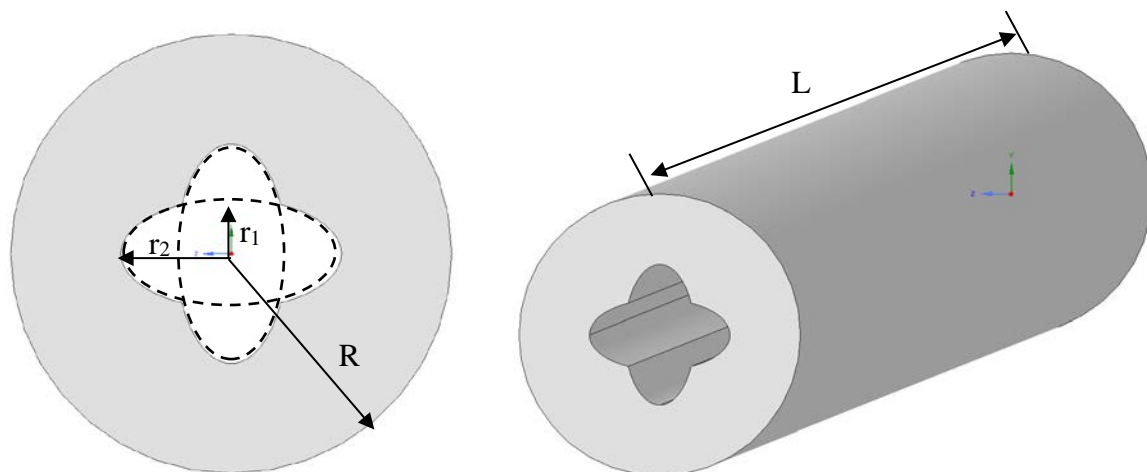

Figure 1. Schematic diagram of the computational domain of annulus.

Pure water, pure ethylene glycol (EG) and water and EG mixtures as the base fluids are selected and the thermophysical properties assumed to be temperature independent. The thermo-physical properties of base fluids and SiO_2 nano particle material used for simulation are shown in Table 1.

Table 1: The thermophysical properties of different nanoparticles and different base fluids at T = 300 K.

Thermo-physical property	Unit	100%W-0%EG	50%W-50%EG	0%W-100%EG	SiO$_2$
Density, ρ	kg/m^3	997,1	1071,1	1132	2200
Specific heat, c$_P$	J/kgK	4180	3300	2349	703
Dynamic viscosity, μ	kg/ms	0,0009	0,0034	0,0151	-
Thermal conductivity, k	W/mK	0,613	0,37	0,258	1,2
Thermal expansion coefficient, β	1/K	0,00021	0,00039	0,00057	0,0000055

Geometry and the governing equations

The phenomenon under consideration is governed by the steady three-dimensional form of the continuity; the time-averaged incompressible Navier–Stokes equations and energy equation are used to describe the heat transfer in the annuals. Heat is transferred between the fluids through the wall which is separating them. Several assumptions were made on the operating conditions of the annulus: (i) the annulus operates under steady-state conditions and three-dimensional; (ii) the nanofluid is Newtonian and incompressible; (iii) the fluid is in single phase and the flow is laminar; (iv) the external heat transfer effects are ignored; (v) the outer walls of the annulus are adiabatic; and (vi) constant thermophysical properties are considered for the nanofluid.

The governing equations for flow and heat transfer in the annulus are as follows (Edition, Ashgriz, & Mostaghimi, 2002):

Continuity equation:

$$\frac{\partial \rho}{\partial t} + \nabla \cdot (\rho \mathbf{v}) = 0 \tag{1}$$

Momentum equation:

$$\rho \frac{D\mathbf{v}}{Dt} = \nabla \cdot \tau_{iJ} - \nabla p + \rho \mathbf{F} \tag{2}$$

Energy equation:

$$\rho \frac{De}{Dt} + \rho \cdot (\nabla \mathbf{v}) = \frac{\partial Q}{\partial t} - \nabla \cdot \mathbf{q} + \Phi \tag{3}$$

Where **v** is the fluid velocity vector, **F** is the body forces, **q** represents heat transfer by conduction and Φ is the dissipation term. These governing equations along with the given boundary conditions are solved to obtain the fluid temperature distribution and pressure drop along the annulus. These data were then used to examine the thermal and flow fields along the annulus.

Boundary conditions

At the elliptic inlet, different velocities depending on the values of Reynolds number were used, and the outlet temperature was taken as T$_{in}$ = 300 K. The constant heat flux used was 100 W/m^2 to heat up the inside walls. At the domain outlet the flow and heat transfer are assumed to be fully developed. The boundary condition can be expressed as follows:

At the inlet of annulus:

$$u_r = u_\theta = u_z = 0 \text{ and } T = T_{in} \tag{4}$$

At the fluid wall interface:

$$u_r = u_\theta = u_z = 0 \text{ and } q_{w,i} = -k_{eff} \frac{\partial T}{\partial r} \tag{5}$$

At the outlet of annulus free pressure outlet is applied:

$p = p_0$ and an overall mass balance correction is applied.

Thermophysical properties of nanofluids

In order to carry out simulations for nanofluids, the effective thermophysical properties of nanofluids must be calculated first. Basically the required properties for the simulations are effective thermal conductivity (k_{eff}), effective dynamic viscosity (μ_{eff}), effective mass density (ρ_{eff}), effective coefficient of thermal expansion (β_{eff}) and effective specific heat (c_{peff}) are given in Table 1. The effective properties of mass density, specific heat and coefficient of thermal expansion are actually calculated according to the mixing theory.

By using Brownian motion of nanoparticles in three-dimensional horizontal concentric annulus, the effect thermal conductivity can be obtained as following mean empirical correlation (Ghasemi & Aminossadati, 2010):

$$k_{eff} = k_{static} + k_{brownian} \tag{6}$$

$$k_{static} = k_f \left[\frac{(k_p + 2k_f) - 2\phi(k_f - k_p)}{(k_p + 2k_f) - \phi(k_f - k_p)} \right] \tag{7}$$

$$k_{brownian} = 5 * 10^4 \beta \phi \rho_f c_{p,f} \sqrt{\frac{\kappa T}{\rho_P d_p}} f(T, \phi) \tag{8}$$

where:

Boltzmann constant: $\kappa = 1.3807 * 10^{-23}$ J/K

Value of the base fluid fraction goes with the nanoparticle, β is calculated as following:

$$\beta_{SiO2} = 1.9526(100\emptyset)^{-1.4594} \quad 1\% \leq \beta \leq 10\% \quad 298 \text{ K} \leq T \leq 363 \text{ K} \tag{9}$$

Modelling function, $f(T, \emptyset)$,

$$f(T, \emptyset) = (2.8217 * 10^{-2} \phi + 3.917 * 10^{-3}) \left(\frac{T}{T_0} \right) + (-3.0669 * 10^{-2} \phi - 3.3911123 * 10^{-3})$$

for $1\% \leq \beta \leq 4\%$ 300 K $\leq T \leq 325$ K
$$\tag{10}$$

By using Brownian motion of nanoparticles the effective viscosity can be obtained by using the following empirical correlation (Mohammed, Abbas, & Sheriff, 2013):

$$\mu_{eff} = \mu_f \frac{1}{\left(1 - 34.87(d_p/d_f)^{-0.3} * \phi^{1.03} \right)}$$

$$d_f = \left[\frac{6M}{N\pi\rho_f} \right]^{1/3} \tag{11}$$

where M is the molecular weigth of base fluid, N is the Avagadro number, $N = 6.022 * 10^{23}$ mol^{-1}, ρ_f is the mass density of the based fluid calculated at temperature $T_0 = 293$ K.

The effective density of the nanofluid can be calculated using (Ghasemi & Aminossadati, 2010):

$$\rho_{eff} = (1 - \phi)(\rho_f) + \phi \rho_p \tag{12}$$

where ρ_{eff} and ρ_{bf} are the nanofluid and base fluid densities respectively and ρ_s is the density of nanoparticle.

The effective specific heat at constant pressure of the nanofluid c_{peff} is computed using the following equation (Ghasemi & Aminossadati, 2010):

$$(\rho c_p)_{eff} = (1-\emptyset)(\rho c_p)_f + \emptyset(\rho c_p)_p \tag{13}$$

where c_{ps} and c_{pbf} are the heat capacity of solid particles and base fluid respectively.

The Nusselt number, the Reynolds number and the friction factor are dimensionless parameters which are calculated, respectively, as follows (Mohammed et al., 2013):

$$Nu = \frac{hD_h}{k_{eff}} \tag{14}$$

where k and h are the thermal conductivity and average heat transfer coefficient of fluid, respectively.

The Reynolds number is defined as:

$$Re = \frac{\rho_{eff} u_m D_h}{\mu_{eff}} \tag{15}$$

where ρ_{eff}, u_m, and μ_{eff} are nanofluid density, mean fluid velocity over the cross section and dynamic viscosity of the nanofluid, respectively.

The hydraulic diameter (D_h) is defined as:

where A is the cross area and P is the wetted perimeter of the cross section.

The friction factor, f, for fully developed flow is expressed as follows:

$$f = \frac{2\Delta p D_h}{L \rho_{eff} u_m^2} \tag{16}$$

and the power required to pump, P, the nanofluid is calculated as follows:

$$P = Q \Delta p \tag{17}$$

where Q is the volumetric flow rate of the nanofluid.

Numerical Solution Method

Grid testing and code validation

The computational domain resulted from the subtraction of the elliptical cylinder section from the circular cylinder section. The grid is made up of triangular elements to improve the quality of the numerical prediction near the curved surfaces.
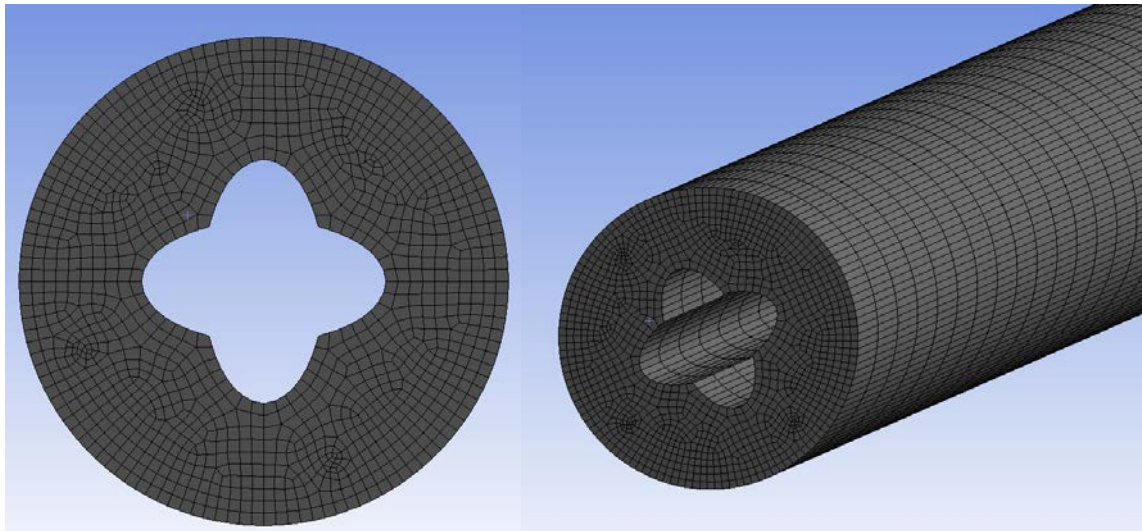
Figure 2. Computational grid of the elliptic annulus.

As shown in Figure 2 the computational grid of the elliptic annulus, built through the mesh generation, three grids types with elements count 153636, 1164822 and 8846771 show no much difference in the values of average Nusselt number and average fanning friction factor. Thus, the grid with 153636 elements is selected in this study as it is found to provide a more stable grid independent solution and due to the fact that resulting in a lower computational cost.

The code validation was done based on the geometry and boundary conditions which were used by (Shah & London, 1978). They studied the thermal characteristics of laminar and turbulent convection heat transfer in a concentric annulus with constant heat flux boundary condition. In this case, the results of the Nusselt number variation were compared with the predictions of the following well-known Shah equation for laminar flows under the constant heat flux boundary condition in the fully developed region as shown in Figure 3. To validate the accuracy of the numerical solutions, the Nusselt number (Nu) and the friction factor times Reynolds number (fRe) of the concentric annular is compared with the theoretical data. It is clearly seen that the deviation between the numerical results and the theoretical data is very low. Therefore, the present numerical predictions have reasonable accuracy.
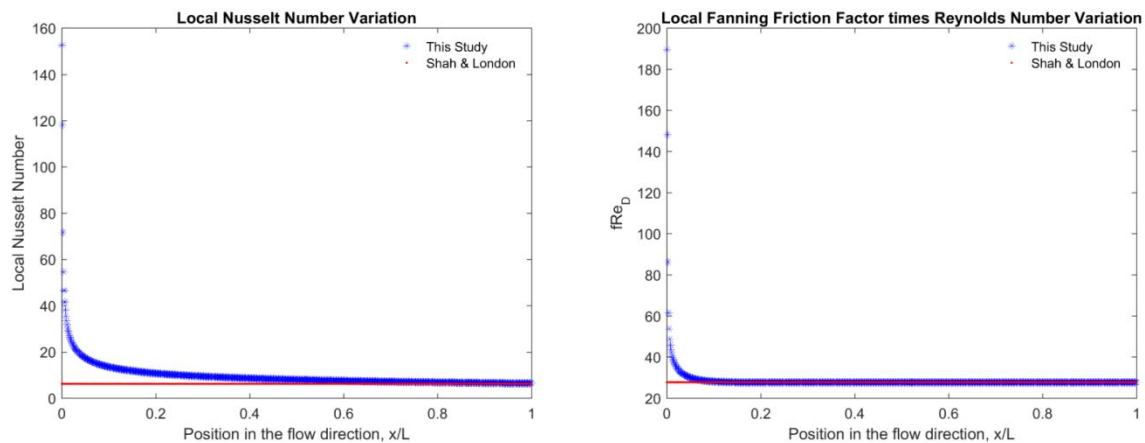

Figure 3. Model comparison Nu (upper) and fRe (lower)

Numerical implementation
A numerical steady-state simulation of the flow field through 3D elliptic concentric annulus is considered to investigate and solve complex fluid flow and heat transfer model. The commercial available CFD software, FLUENT was used to solve the governing equations of continuity, momentum and energy. The numerical computations were performed by solving the governing conservations along with the boundary conditions using the finite volume method (FVM). It is based on the control volume method; COUPLED algorithm is used to deal with the problem of velocity and pressure coupling. The pressure staggering option (second order) scheme is used to solve pressure equations. The diffusion term in the momentum and energy equations was approximated by second-order central difference which gives a stable and more accurate solution. In addition, a second-order

upwind differencing scheme was adopted for the convective terms (John & Anderson, 1995). The numerical model was developed in the physical domain, and dimensionless parameters were calculated from the computed velocity and temperature distributions. The residual sum for each of the conserved variables is computed and stored at the end of each iteration. The convergence criterion required that the maximum relative mass residual based on the inlet mass be smaller than 1×10^{-5}. Also average Nusselt number and fanning friction factor values were watched through the simulations to decide the convergence of the solution as their value not to change after a certain value.

Results and Discussion

The simulations are performed of laminar forced convection heat transfer and fluid flow for different types of base fluids in a three-dimensional through a double-integrated elliptic annulus. Effect of water and ethylene glycol volume fractions are addressed as EG fractions ranges from 0% to 100% with a 50% increment. Different values of Reynolds number were used in the range of $200 \leq \text{Re} \leq 1000$ for laminar flow and with volume friction of SiO_2 nanoparticles in the range of $0 \leq \phi \leq 0.04$ with a diameter of 20 nm. Nanofluids are proven to enhance the heat transfer characteristics. However, there is no research done on finding the effect of the base fluid. To get the best base fluid, each base fluid is compared in terms of average surface Nusselt number and pumping power.

Effect of different volume fractions of nanoparticles

In this section, the effect of nanoparticles volume fraction on the average Nusselt number was investigated in the range of 0–4% with different values of the Reynolds number and diameter of particle d_p =20 nm for SiO_2 nanofluid. As shown clearly in

Figure 4, increasing nanoparticle volume fraction enhances the Nusselt number. The Nusselt number is not very sensitive to the volume fraction of nanoparticles at lower Reynolds number and in all cases with increasing the Reynolds number, the Nusselt number increases. It can be seen that the highest
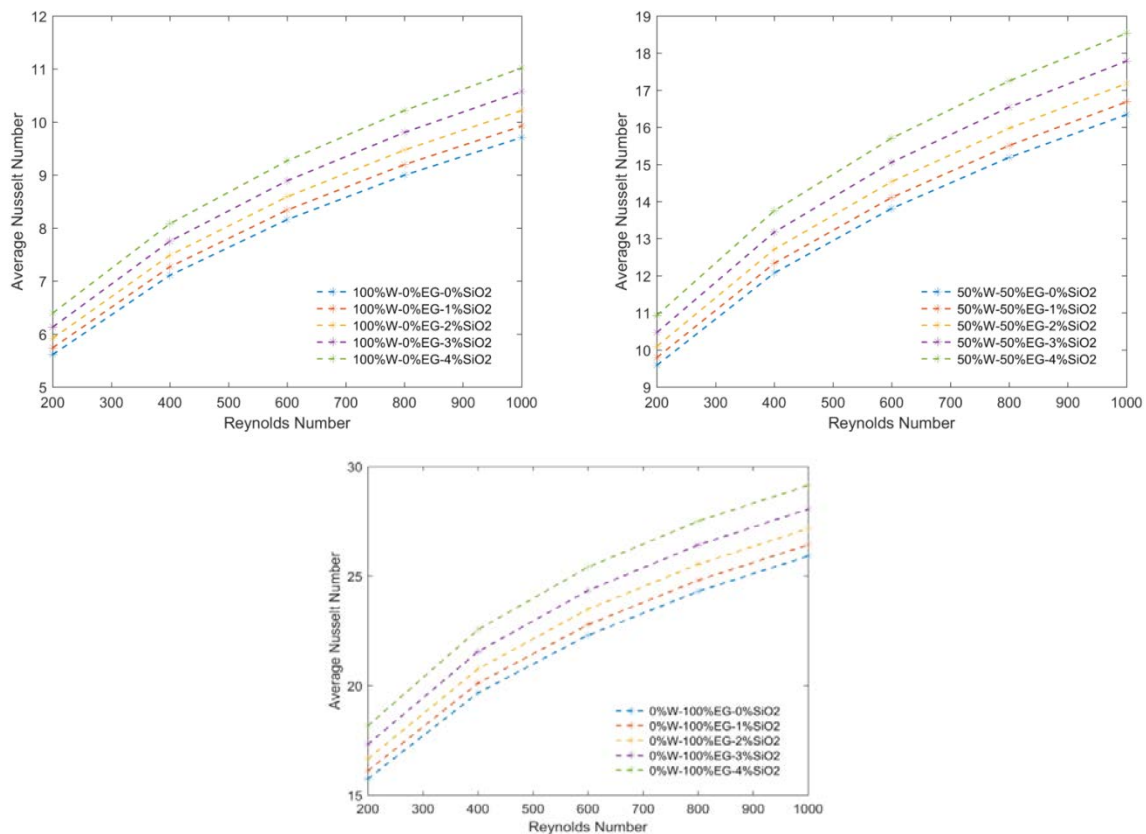

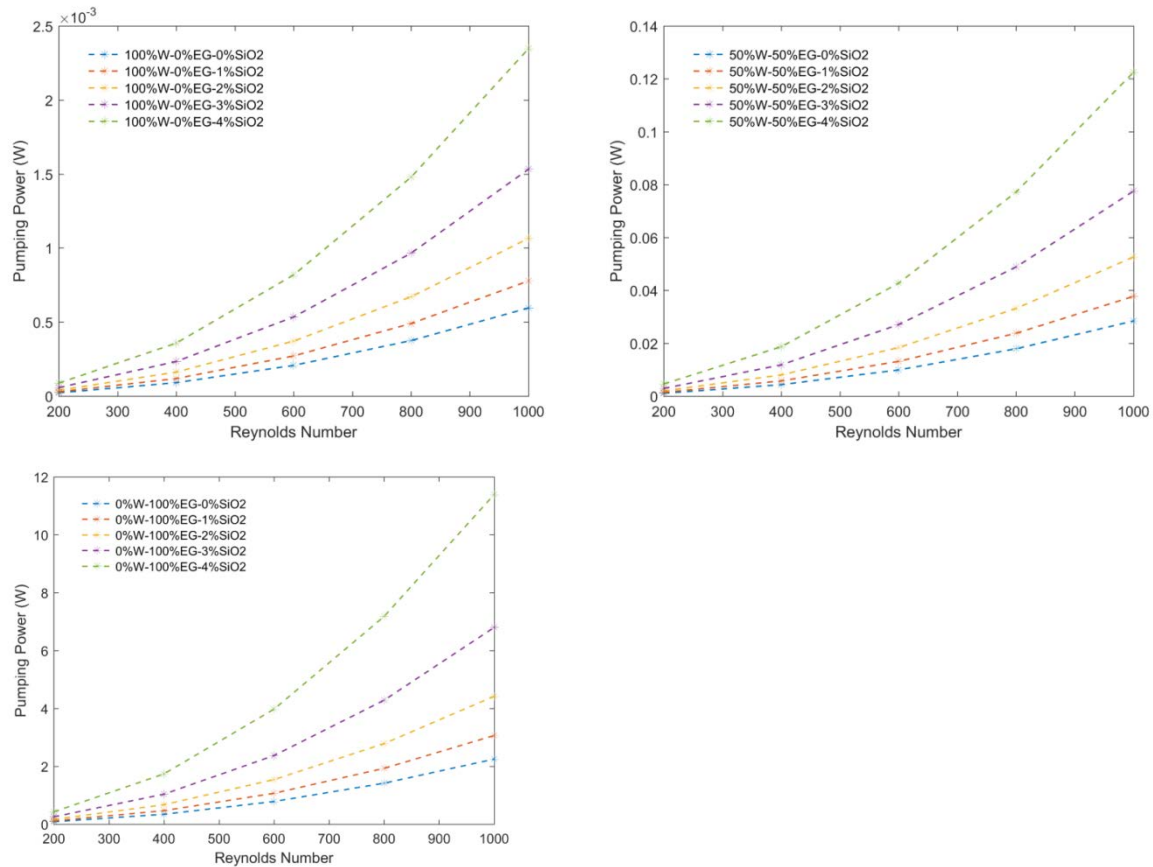**Figure 4.** Average Nusselt Number variations due to effect of nanoparticle volume fraction

Figure 5. Average Nusselt Number variations due to effect of nanoparticle volume fraction

concentration of nanoparticles has the highest Nusselt number profiles. This is due to the enhanced effective thermal conductivity of the nanofluid which is accompanied by an increase in the thermal diffusivity. Heat transfer enhancement is increased when volume fraction is increased; it can be observed that 4% volume fraction has the highest heat transfer enhancement, while 0% concentration has the lowest enhancement as shown in

Figure *4*. This is because the physical properties of nanofluid vary with the volume fraction. Thus, transfers more energy in the fluid, because of the momentum energy is much higher than the thermal energy in higher volume fraction.

As illustrated in Figure 5, the pumping power increases with the increase of Reynolds number for different volume fractions of nanoparticles. In general, the increase of nanoparticles volume fraction results in an increase of fluid viscosity which diminishes the fluid movement.
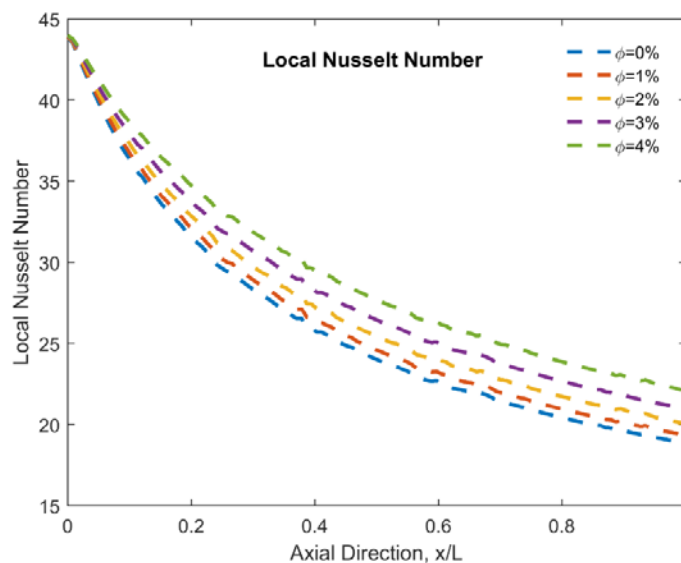
Figure 6. Local Nusselt Number variations due to effect of different volume fractions

Figure 6 shows the variation of the local Nusselt numbers through the annulus with Reynolds number chosen as 1000 and pure EG is the base fluid with different SiO_2 particle volume fractions. Local heat transfer coefficients thus the local Nusselt numbers values are very high at the entrance since the flow is developing. Because the thickness of the thermal boundary layer is zero at the entrance and it decreases continuously in the axial direction due to the thermal boundary layer that develops. As illustrated, when the nanoparticle concentration increases, local Nusselt number values also increases since the Brownian motion that dissipates heat is higher at high nanoparticle concentrations.

Velocity distribution and isotherms contours at the outlet of the annulus for pure EG nanofluid with different SiO_2 particle volume fraction at Reynols number value equals to 1000 have been shown in Figure 7. The left hand side of the figure shows the isoterms while rigth hand side shows the velocity distribution. In this case local Nusselt Numbers varies as 18.87, 19.35, 20.08, 20.97 and 22.11 for volume fractions %0, 1, 2, 3 and 4, respectively. Thus there is no much difference and this is also supported by isoterms since they seem to be nearly the same for all concentrations. By adding the nanoparticle, that is by increasing the nanoparticle volume concentration, both density and dynamic viscosity of nanofluid increases. However ratio of density and dynamic viscosity decreases with increasing concentration. Velocities at the annulus walls are zero for all cases due to the boudary layer that develops. Therefore for the same Reynolds number values, the nanofluid with the highest concentration has the highest velocity in the annulus core. This fact is also supported by the velocity contours which are shown. As the intensity of red color increaes that means that the velocity also increases. There are also local increments in the velocities where the length is lower between the inner and outer walls due to narrowing crosssection in this regions.
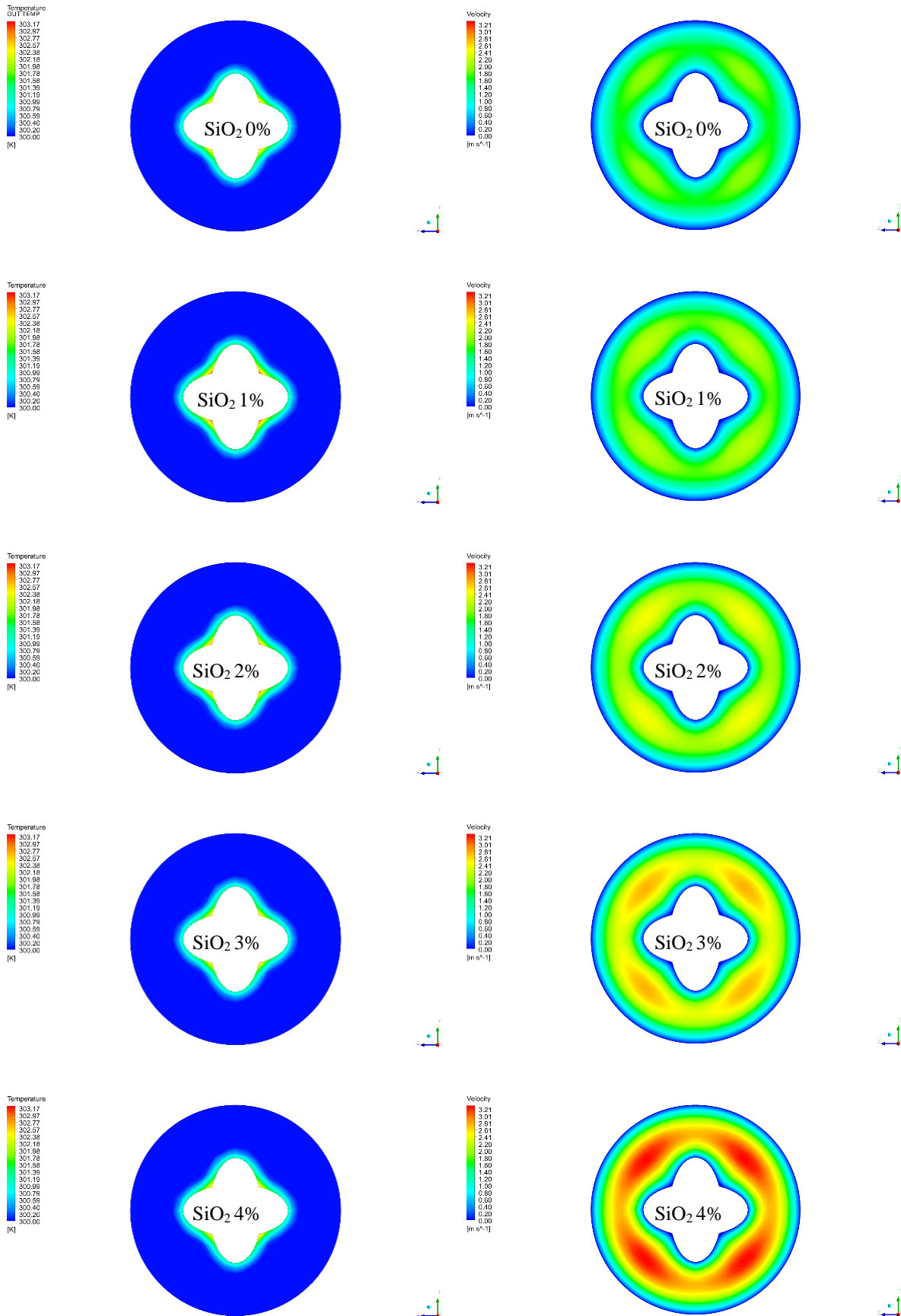
Figure 7. Isotherms (left) contours and velocity distribution (rigth) and for varying volume fractions

Conclusion

Numerical simulations for laminar forced convection heat transfer and fluid flow characteristics in a double integrated elliptic annulus using various nanofluids as the working fluids were presented. A three dimensional grid setup was built in order to simulate the geometry using Computational Fluid Dynamics (CFD) software. Using finite volume method (FVM), the governing equations were deciphered and correlated to case study, provided with some particular assumptions. The emphasis is given on the heat transfer enhancement resulting from various parameters, which include base fluid types and volume fraction of nanoparticle. The results were obtained through the numerical simulation that gives the highest Nusselt number. It is found that SiO_2 EG nanofluid gives the highest Nusselt number while pure water gives the lowest Nusselt number. The Nusselt number is remarkably increased with the increments of nanoparticle volume fraction and Reynolds number. However use of EG in such microchannels sharply increases the required pumping power. This may be a drawback for this nanofluid if there is no available space for larger size pumps.

References

Akbarinia, A. (2008). Impacts of nanofluid flow on skin friction factor and Nusselt number in curved tubes with constant mass flow. *International Journal of Heat and Fluid Flow*, *29*(1), 229–241. https://doi.org/10.1016/j.ijheatfluidflow.2007.05.003

Akbarinia, A., & Behzadmehr, A. (2007). Numerical study of laminar mixed convection of a nanofluid in horizontal curved tubes. *Applied Thermal Engineering*, *27*(8–9), 1327–1337. https://doi.org/10.1016/j.applthermaleng.2006.10.034

Choi, S. U. S., 1995. (n.d.). "Enhancing Thermal Conductivity of Fluids With Nanoparticles," Developments and Applications of Non-Newtonian Flows, Report No. FED-231/MD-66.

Dawood, H. K., Mohammed, H. A., Sidik, N. A. C., & Munisamy, K. M. (2015). Numerical investigation on heat transfer and friction factor characteristics of laminar and turbulent flow in an elliptic annulus utilizing nanofluid. *International Communications in Heat and Mass Transfer*, *66*, 148–157. https://doi.org/10.1016/j.icheatmasstransfer.2015.05.019

Edition, S., Ashgriz, N., & Mostaghimi, J. (2002). *An introduction to computational fluid dynamics. Fluid flow handbook. McGraw-Hill …* (Vol. M). Retrieved from http://www.mie.utoronto.ca/labs/mussl/cfd20.pdf

Ghaffari Motlagh, Y., Ahn, H. T., Hughes, T. J. R., & Calo, V. M. (2013). Simulation of laminar and turbulent concentric pipe flows with the isogeometric variational multiscale method. *Computers and Fluids*, *71*, 146–155. https://doi.org/10.1016/j.compfluid.2012.09.006

Ghasemi, B., & Aminossadati, S. M. (2010). Brownian motion of nanoparticles in a triangular enclosure with natural convection. *International Journal of Thermal Sciences*, *49*(6), 931–940. https://doi.org/10.1016/j.ijthermalsci.2009.12.017

Izadi, M., Behzadmehr, A., & Jalali-Vahid, D. (2009). Numerical study of developing laminar forced convection of a nanofluid in an annulus. *Int J Therm Sci*, *48*, 2119–2129.

John, D., & Anderson, J. R. (1995). *Computational fluid dynamics: the basics with applications. P. Perback, International ed., Published*.

Joye, D. D. (2003). Pressure drop correlation for laminar , mixed convection , aiding flow heat transfer in a vertical tube, *24*, 260–266. https://doi.org/10.1016/S0142-727X(02)00238-2

Keblinski, P., Phillpot, S., Choi, S., & Eastman, J. (2002). Mechanisms of heat flow in suspension of nanosized particles (nanofluids). *International Journal of Heat and Mass Transfer*, *45*, 855–863.

Khaled, A. R. A. (2007). Heat transfer enhancement in hairy fin systems. *Applied Thermal Engineering*, *27*(1), 250–257. https://doi.org/10.1016/j.applthermaleng.2006.04.012

Lee, S., Choi, S. U.-S., Li, S., & Eastman, J. A. (1999). Measuring Thermal Conductivity of Fluids Containing Oxide Nanoparticles. *Journal of Heat Transfer*, *121*(2), 280. https://doi.org/10.1115/1.2825978

Masuda, H., Ebata, A., & Teramae, K. (1993). Alteration of thermal conductivity and viscosity of liquid by dispersing ultra-fine particles. *Netsu Bussei*, *7*(4), 227–233. Retrieved from http://en.journals.sid.ir/ViewPaper.aspx?ID=312989

Mirmasoumi, S., & Behzadmehr, A. (2008). Numerical study of laminar mixed convection of a nanofluid in a horizontal tube using two-phase mixture model. *Applied Thermal Engineering*, *28*(7), 717–727.

Mohammed, H. A., Abbas, A. K., & Sheriff, J. M. (2013). Influence of geometrical parameters and forced

convective heat transfer in transversely corrugated circular tubes. *International Communications in Heat and Mass Transfer*, *44*, 116–126. https://doi.org/10.1016/j.icheatmasstransfer.2013.02.005

Mokhtari Moghari, R., Akbarinia, A., Shariat, M., Talebi, F., & Laur, R. (2011). Two phase mixed convection Al2O3-water nanofluid flow in an annulus. *International Journal of Multiphase Flow*, *37*(6), 585–595. https://doi.org/10.1016/j.ijmultiphaseflow.2011.03.008

Sakalis, V. D., Hatzikonstantinou, P. M., & Kafousias, N. (2001). Thermally developing flow in elliptic ducts with axially variable wall temperature distribution. *International Journal of Heat and Mass Transfer*, *45*(1), 25–35. https://doi.org/10.1016/S0017-9310(01)00124-7

Shah, R. K., & London, A. L. (1978). *Laminar Flow Forced Convection in Ducts*. *Laminar Flow Forced Convection in Ducts*. https://doi.org/10.1016/B978-0-12-020051-1.50022-X

Shoji, Y., Sato, K., & Oliver, D. R. (2003). Heat transfer enhancement in round tube using wire coil: Influence of length and segmentation. *Heat Transfer?Asian Research*, *32*(2), 99–107. https://doi.org/10.1002/htj.10072

Velusamy, K., & Garg, V. K. (1996). Laminar mixed convection in vertical elliptic ducts. *International Journal of Heat and Mass Transfer*, *39*(4), 745–752. https://doi.org/10.1016/0017-9310(95)00163-8

Velusamy, K., Garg, V. K., & Vaidyanathan, G. (1995). Fully developed flow and heat transfer in semi-elliptical ducts. *International Journal of Heat and Fluid Flow*, *16*(2), 145–152. https://doi.org/10.1016/0142-727X(94)00019-9

Wang, X. W., Xu, X. F., & Choi, S. U. S. (1999). Thermal conductivity of nanoparticle-fluid mixture. *Journal of Thermophysics and Heat Transfer*, *13*(4), 474–480. https://doi.org/10.2514/2.6486

Xuan, Y. (2000). Heat transfer enhancement of nanofluids, 7.

Xuan, Y., & Roetzel, W. (2000). Conceptions for heat transfer correlation of nano ¯ uids, *43*, 3701–3707. https://doi.org/doi.org/10.1016/S0017-9310(99)00369-5

Zimparov, V. (2001). Enhancement of heat transfer by a combination of three-start spirally corrugated tubes with a twisted tape. *International Journal of Heat and Mass Transfer*, *44*(3), 551–574. https://doi.org/10.1016/S0017-9310(00)00126-5